Supporting Information

New insights on the substantially reduced bandgap of bismuth layered perovskite oxide thin films

Mohammad Moein Seyfouri[1†], Qianluan Liu[1†], Jack Yang[1*], Yunlong Sun[1], Xinchen Dai[1],

Junjie Shi[1], Xin Tan[2], Sean Li[1], Tom Wu[1] and Danyang Wang[1*]

[1] *School of Materials Science and Engineering, The University of New South Wales, Sydney, NSW 2502, Australia*

[2] *Integrated Materials Design Laboratory, Department of Applied Mathematics, Research School of Physics, The Australian National University, Canberra, ATC 2601, Australia*

[†]These authors contributed equally.

*Corresponding authors: JY: jianliang.yang1@unsw.edu.au, DW: dy.wang@unsw.edu.au

Figure S1 shows the secondary electrons (SE) and back-scattered electrons (BSE) images of the cross-sectional view of the BLT films deposited on STO (001). All images were obtained at 200 000× magnification using FEI (Thermo Fisher) Nova NanoSEM 450 Microscopy. The clear sections of the substrates are seen in the SE image, indicating that samples are continuous with a dense and firm interface between film and substrate. The thickness of the film was determined to be ~215 nm via Nova NanoSEM software. The contrast in Back-scattered electrons image clearly distinguishes thin film and the substrate, since the back-scattered electrons are sensitive to the atomic mess of the atoms, the brighter layer represents the deposited film consisting of the Bi and La that scatter the electrons more efficiently compared to constituent atom of substrate.
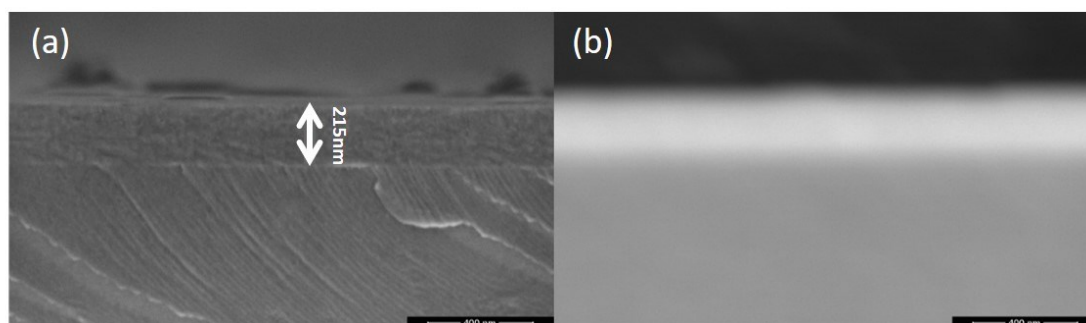

Figure S1 (a) Cross-section SEM SE images. (b) corresponding BSE images of BLT film.

High-resolution XPS region scans were acquired to investigate the valence state of the constituent in the BLCT thin film. The core-level photoemission of Bi-4f, Ti-2p, Co-2p and O-1s are shown in Figure S2. The principal peaks of Bi-4f core level are located at 159 and 164.3 eV corresponding to binding energy of the $4f_{7/2}$ and $4f_{5/2}$, respectively. The spin-orbit doublets of Bi-4f are separated by 5.3 eV, indicating Bi^{+3} formal oxidation state consistent with Bi_2O_3 spectrum.[1] As seen in Figure S2(b), the Ti-$2p_{3/2}$ peak can be clearly located as a distinctive feature at the binding energy of 458 eV, very similar to that of tetravalent titanium atoms within perovskite titanates.[2] This finding unambiguously confirms our earlier assumption in DFT calculation regarding the formation of an oxygen vacancy in the vicinity of Bi_2O_2 layer rather than in the perovskite-like $Bi_2Ti_3O_{10}$ layer. To clarify the valence state of cobalt ions, the photoemission spectrum of Co-2p was investigated (see Figure S2(c)). The region scan around Co-2p spectrum exhibits $2p_{1/2}$ and $2p_{3/2}$ component and since both contain similar chemical information, the more pronounced $2p_{3/2}$ profile was fitted for further analysis. Cobalt oxides, i.e. Co_2O_3, CoO and Co_3O_4, have almost identical binding energy and therefore the valence state of cobalt cannot be resolved promptly unless the intensity and separation of satellite peaks are considered. The prominent fitted curve at lower binding energy with corresponding weak satellite feature at 788.7 eV represents Co^{3+}. Whilst, according to the intensity ratio of satellite for CoO reported earlier,[3] the other peak at higher energy level coupled with the more intense satellite peak at 786 eV corresponds to Co^{2+}. The higher intensity ratio of the shake-up and its main peak ($2p_{3/2}$) is characteristic of the charge-transfer band structure related to the 3d transition metal monoxides, e.g. CoO.[4] The observed lineshape suggests the coexistence of cobalt ion in the mixed-valence state of +2/+3, with trivalent cobalt being the majority (Co^{3+}:Co^{2+} ratio of approximately 1.5:1). Furthermore, the clear peaks at lower energy side of O-1s spectrum can be associated with transition metal-O species (e.g. Co-O) in accord with the photoelectron line position of these compounds.[5] However, the precise determination of various Co-O environment is subtle since the difference in their line position in the O-1s spectrum is in the limit of 0.5 eV.[6]
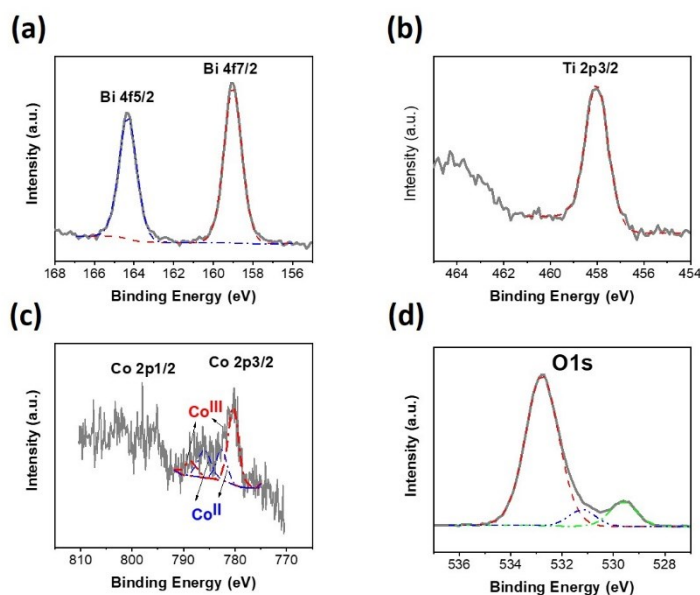

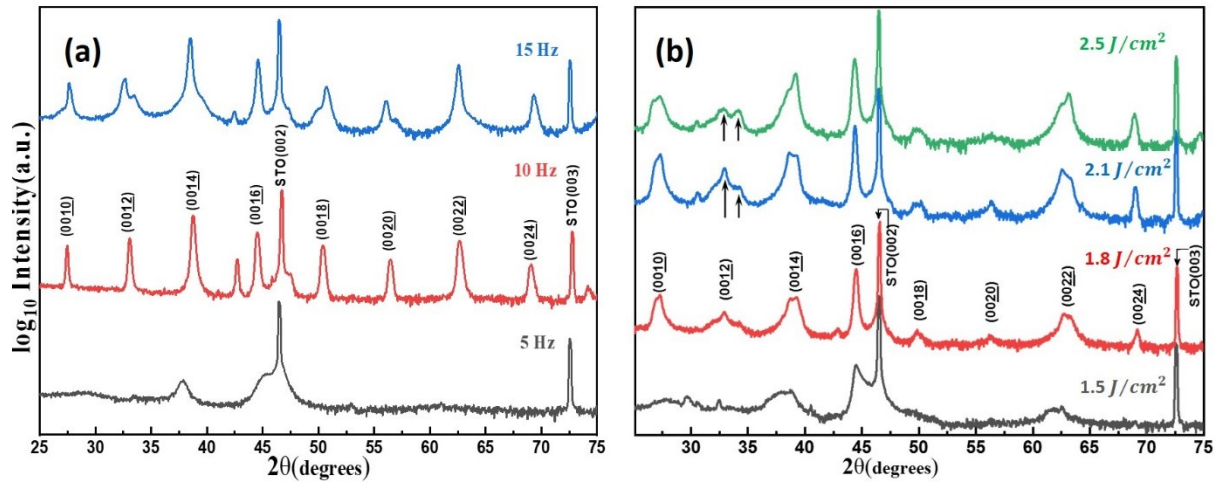**Figure S2** High resolution XPS scan (a) Bi-4f (b) Ti-2p (c) Co-2p (d) O-1s.

Figure S3 Broad X-ray diffraction pattern of (a) c-axis oriented BLT thin films deposited at different laser repetition rates. (b) c-axis oriented BLFT thin films deposited using different laser energy density (The splitting of (0012) peaks are denoted by arrows)
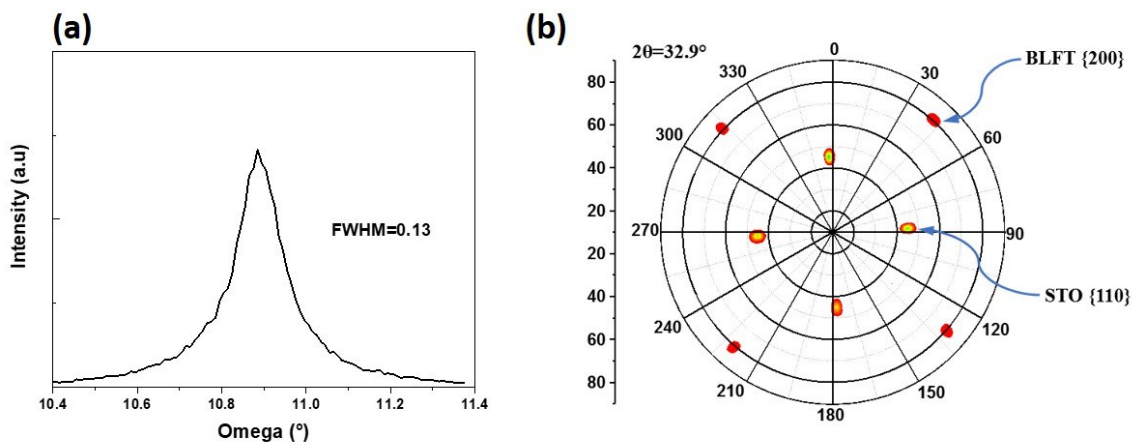

Figure S4 (a) Rocking curve of (008) diffraction peak and (b) XRD pole figure of BLFT thin films grown on STO (001)

The surface morphology of the films varies considerably by incorporation of the dopants into BLT lattice. As shown in Figure S5, the smallest RMS surface roughness was obtained for BLT films with a value of 0.95 nm. The surface roughness significantly increases to ~4.0 and 9.8 nm for BLFT and BLCT thin films, respectively. Distinctive pyramid-shaped islands are clearly detectable on the surface of BLFT thin film, as shown in Figure S5(b), demonstrating the growth of BLFT films is governed by the Vollmer-Weber mode. This typical 3D island formation was observed previously for c-axis oriented films of $Bi_2O_2(A_{n-1}B_nO_{3n+1})$ Aurivillius family due to the large lattice mismatch

between this complex oxide and the substrate.[7] Brown et al. have conducted a more detailed study on the surface morphology of (001) BiT film grown on STO, showing the growth mechanism is actually in Stranski-Krastonov mode, in which a transition to the 3D island growth mode occurs upon strain relaxation at the critical thickness.[8] It is noteworthy to point out that the vertical distance between the two steps of the island is about 3.7 nm which corresponds to the c-axis lattice parameter of BLFT films (see Figure S5(d)). The formation of the steps on the pyramid-shaped islands can be attributed to the preferred spiral columnar growth of c-axis oriented films because of the higher growth rate of c-plane to that of a/b-plane. [9,10] Furthermore, as shown in Figure S5(c), the average RMS roughness of BLCT films was considerably larger than BLFT and BLT. In contrast to the BLFT and BLT films, unique squared-shape features appear on the surface of BLCT films, which induces the rougher surface.
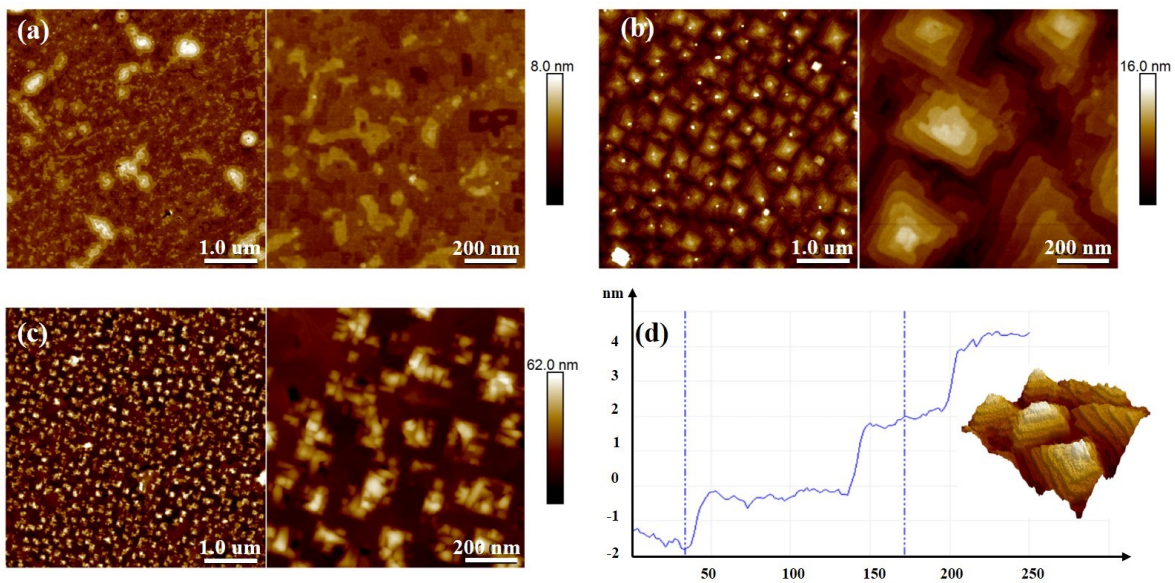

Figure S5 AFM images of (a) BLT (b) BLFT (c) BLCT thin films. (d) 3D image of pyramid-shaped island for BLFT thin film along with the depth profile of island generated by NanoScope Analysis software
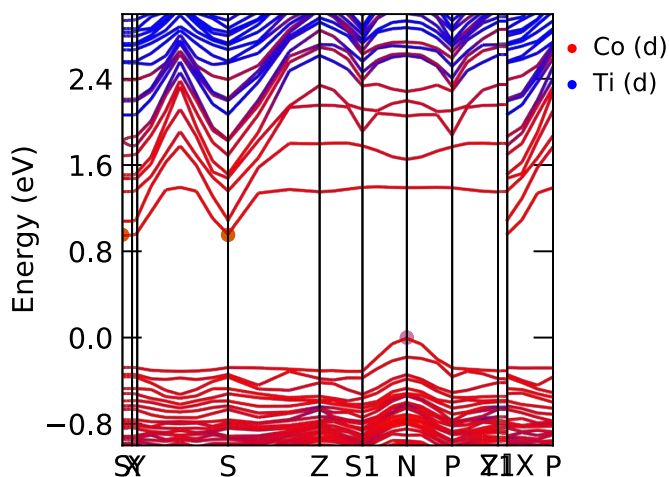
Figure S6 Spin non-polarized electronic band structures of $Bi_{3.25}La_{0.75}Co_1Ti_2O_{11.5}$, showing indirect nature of bandgap

References

1. J. Liang, G. Zhu, P. Liu, X. Luo, C. Tan, L. Jin and J. Zhou, Synthesis and characterization of Fe-doped β-Bi_2O_3 porous microspheres with enhanced visible light photocatalytic activity, *Superlattices Microstruct.*,2014, 72, 272–282.

2. M. Murata, K. Wakino and S. Ikeda, X-ray photoelectron spectroscopic study of perovskite titanates and related compounds: An example of the effect of polarization on chemical shifts, *J. Electron Spectros. Relat. Phenomena*,1975, 6, 459–464.

3. Y. Okamoto, H. Nakano, T. Imanaka and S. Teranishi, X-Ray Photoelectron Spectroscopic Studies of Catalysts-Supported Cobalt Catalysts-, *Bull. Chem. Soc. Jpn.*,1975, 48, 1163–1168.

4. G.A. Carson, M.H. Nassir and M.A. Langell, Epitaxial growth of Co_3O_4 on CoO(100) , *J. Vac. Sci. Technol. A Vacuum, Surfaces, Film.*,1996, 14, 1637–1642.

5. J.F. Moulder, W.F. Stickle, P.E. Sobol and K.D. Bomben, Handbook of X-Ray Photoelectron Spectroscopy, Perkin-Elmer Corporation, Eden Prairie, 1993.

6. K. Artyushkova, S. Levendosky, P. Atanassov and J. Fulghum, XPS Structural studies of nano-composite non-platinum electrocatalysts for polymer electrolyte fuel cells, *Top. Catal.*, 2007, 46, 263–275.

7. N. Deepak, P. Carolan, L. Keeney, M.E. Pemble and R.W. Whatmore, Tunable nanoscale structural disorder in Aurivillius phase, n = 3 $Bi_4Ti_3O_{12}$ thin films and their role in the transformation to n = 4, $Bi_5Ti_3FeO_{15}$ phase, *J. Mater. Chem. C*, 2015, 3, 5727–5732.

8. G.W. Brown, M.E. Hawley, C.D. Theis, J. Yeh and D.G. Schlom, Atomic force microscopy examination of the evolution of the surface morphology of $Bi_4Ti_3O_{12}$ grown by molecular beam epitaxy, *Thin Solid Films*, 1999, 357, 13–17.

9. M. Hawley, I.D. Raistrick, J.G. Beery and R.J. Houlton, Growth mechanism of sputtered films of $YBa_2Cu_3O_7$ studied by scanning tunneling microscopy, *Science*, 1991, 251, 1587–1589.

10. N. Zhong and T. Shiosaki, C-axis-oriented $Bi_{3.25}La_{0.75}Ti_3O_{12}$ ferroelectric thin film fabricated by chemical solution deposition, *Mater. Lett.*, 2007, 61, 2935–2938.